## Vibration Control of a Structure and a Rotor Using One-sided Magnetic Actuator and a Digital Proportional-derivative Control


A. Nandi, S. Neogy and H. Irretier



*Journal of Vibration and Control* 2009 15: 163

DOI: 10.1177/1077546307085212

# Vibration Control of a Structure and a Rotor Using One-sided Magnetic Actuator and a Digital Proportional-derivative Control

A. NANDI
S. NEOGY
*Department of Mechanical Engineering, Jadavpur University. Kolkata 700 032, India (arghyan@yahoo.com)*

H. IRRETIER
*Institute for Mechanics, University of Kassel, Kassel, Germany*

(Received 19 March 2007; accepted 21 August 2007)

*Abstract:* The present work aims at vibration control of a structure/rotor using a one-sided magnetic actuator. For such an actuator, the actuator force is a nonlinear function of current through the coil of the actuator and the gap between the actuator and the structure/rotor. Though the actuator introduces sufficient nonlinearity to the system, it has the advantage that, for applying force in a direction, this actuator needs to be placed in only one side of the structure/rotor. For vibration control of the structure/rotor, a simple digital proportional derivative (PD) control technique is suggested here. It is considered that the displacement signal from the sensor is sampled at specific instants of time and a series of discrete values of displacement is made available to the digital controller. The controller processes the above values of displacement to compute the values of control current that produces the values of appropriate control force at the corresponding instants. The input current to the actuator is kept constant between two consecutive sampling instants. The response of the controlled system (the structure/rotor along with the digital controller) is computed using standard time-marching algorithms (with time steps much smaller than the sampling interval). The effect of the sampling interval in the response pattern is observed for a single-degree-of-freedom (SDOF) system, a finite element model of a beam and a four degree-of-freedom model of a rotor.

*Keywords:* Magnetic actuator, rotor, finite element, and digital PD control.

## 1. INTRODUCTION

Magnetic actuators are extensively used in magnetic bearings for magnetic levitation and vibration control of rigid body and flexible modes of a rotor. Much research has already been done on design and application of magnetic actuators for magnetic bearings (Schweitzer et al., 2003; Genta, 2004; Chiba et al., 2005).

In magnetic actuator configuration, two counteracting electromagnets are generally used to apply force in a direction. The structure/rotor is placed in between the two counteracting

*Journal of Vibration and Control,* **15(2):** 163–181, 2009 DOI: 10.1177/1077546307085212

Figures 4, 5, 7, 9–12 appear in color online: http://jvc.sagepub.com

magnets. This configuration allows the actuator to apply both positive and negative force in that direction. Generally, a bias current passes through the coils of both the counteracting magnets. Ideally, when equal current flows through the counteracting magnets, no force acts on the structure/rotor. If the current in one of the magnets increases by an amount above the bias current and decreases by the same amount below the bias current in the other one, then it is possible to get a linearized force-current relationship for the actuator.

Due to space constraints it may be difficult to place counteracting pairs of magnets around a structure/rotor already in operation. It would be much easier if force in one direction could have been applied using magnet(s) from one side alone in place of a counteracting pair with the structure/rotor in between. Because a magnet can only pull, in this case, an initial static pulling force must be applied to the structure/rotor by a static current to cause a static deflection of the structure/rotor. For vibration control of the structure/rotor, a varying control current needs to be algebraically added to this initial static current. However, this actuator necessarily becomes more nonlinear compared to its counteracting counterpart, especially when the displacement of the structure/rotor at the location of the actuator becomes a comparatively large fraction of the gap between the two.

The present work explores the possibility of designing such a one-sided actuator for vibration control of a structure/rotor. Such a one-sided magnetic exciter for vibration excitation of structures and rotors has already been developed and reported on (Kreuzinger-Janik and Irretier, 2000a,b). In the present work a similar actuator is considered along with a digital controller for the purpose of vibration control of a structure/rotor.

A digital controller is much more flexible than its analog counterpart. In a digital controller, a change in the control strategy or control parameter requires only an appropriate change in the software. For a similar change in an analog controller, changes are to be incorporated in the hardware level and it calls for an expert in analog electronics. Nowadays, with the advancement of processor technology, inexpensive digital controllers are easily available. Considering the above reasons, a digital controller comes out an obvious choice for the purpose of the present investigation.

An accurate simulation of a structure/rotor with the above one-sided actuator and digital proportional derivative controller is required to assess the performance of the actuator. An analog controller continuously changes the control input to the structure depending on the response of the structure and the control strategy adopted. For this reason, analog control is also known as a continuous-time control. Unlike its analog counterpart, a digital controller works on a series of discrete values made available to it by the analog to digital converter (ADC). The discrete values are collected at a constant interval of time known as the sampling interval. After processing the discrete values according to the control technique used, the controller outputs the control signal via a digital to analog converter (DAC) using a zero order hold (ZOH). Therefore, the control signal, computed at a sampling instant, remains constant till the next sampling instant. In this work, a voltage to current converter converts the voltage signal (from the DAC) to current. This current passes through the actuator coil. An ideal voltage to current converter faithfully follows the voltage pattern. Chiba et al. (2005) discussed the working principles for such a power amplifier in considerable detail. As a consequence, the input current to the actuator is of a staircase type. This staircase type of current can be accurately modeled using a time marching algorithm with time steps much smaller than the sampling interval.

In the present work, the plant, i.e., the structure/rotor is of continuous-time type and the controller is digital. The plant responds continuously depending on its inputs and states while the controller works on a series of digital values. Within a sampling interval the input to the actuator is constant but the actuator force continuously varies as the gap between the actuator and the structure continuously changes. Moreover, the actuator force is largely dependent on this changing gap. At a particular instant of time one does not know the value of actuator force unless the gap is computed at that instant. On the other hand the gap depends on the actuator force. This nonlinear actuator force needs to be modeled appropriately.

Selecting the correct sampling time is of central importance for digital control. Intuitively, a short sampling time always seems a good idea because it is closer to continuous time (which can be thought of as infinitely short sampling time). This is not necessarily the case. In standard analysis of a continuous plant with a digital control system, including the present one, a staircase-type signal is considered as a series of step signals with different magnitude and starting time. However, this assumption is true only when the sampling time is much larger compared to the reaction time of the controller. The reaction time is the time between the start of accepting the input by the ADC from the sensor and the end of output of the control signal from the DAC. It includes the analog to digital and digital to analog conversion times plus the time required for computations. If a very small sampling time is used, the reaction time can become a considerable fraction of the sampling time. If this is so, the control system will not behave in the way it is designed for. Therefore, for a very small sampling time a faster digital controller needs to be used, which obviously increases the expense.

One of the objectives of the present work is to assess, at least approximately, the maximum sampling time that can be used for the specific purpose. There are some thumb rules for assessing the sampling time for linear time invariant (LTI) systems (Gopal, 2003). However, these are not expected to be valid in the present case as the actuator makes the present system sufficiently nonlinear. The present numerical simulation is believed to be useful in determining, by a trial and error method, an appropriate sampling time that produces a satisfactory response of the structure/rotor.

## 2. ANALYSIS

### *2.1. The Model of Structure and Rotor*

The dynamic equilibrium of the structure/rotor at an instant of time $t$ is represented by the following set of ordinary differential equations:

$$[M]\left\{\ddot{Y}(t)\right\} + [D]\left\{\dot{Y}(t)\right\} + [K]\{Y(t)\} = \{T_d\}\, f_d(t) + \{T_c\}\, f_c(t)\,. \tag{1a}$$

Where, $[M]$ and $[K]$ are mass and stiffness matrices respectively

For a structure, $[D] = [C]$

For a finite element model the damping matrix $[C]$ may be determined using the Rayleigh damping model.

For a rotor, $[D] = [G] + [C]$

The matrix $[C]$, as in the case of structures, has contributions only from damping where, the matrix $[G]$ is the anti-symmetric gyroscopic matrix.

The disturbing force along a single degree-of-freedom is denoted by $f_d(t)$ and the control force, also considered along a single degree-of-freedom, is denoted by $f_c(t)$. The vectors $\{T_d\}$ and $\{T_c\}$ relates the disturbing and control force along a single degree-of- freedom to all the degrees-of-freedom of the system and can be termed as disturbance influence matrix and control influence matrix respectively.

Equation (1a) can also be expressed in the following first order form:

$$\{\dot{z}(t)\} = [A]\{z(t)\} + \{B_d\}u_d(t) + \{B_c\}u_c(t) \tag{1b}$$

where,

$$\{z(t)\} = \begin{Bmatrix} \{\dot{Y}(t)\} \\ \{Y(t)\} \end{Bmatrix} \quad [A] = \begin{bmatrix} -[M]^{-1}[D] & -[M]^{-1}[K] \\ [I] & [0] \end{bmatrix}$$

$$\{B_d\} = \begin{Bmatrix} [M]^{-1}\{T_d\} \\ \{0\} \end{Bmatrix} \quad \{B_c\} = \begin{Bmatrix} [M]^{-1}\{T_c\}\pi \\ \{0\} \end{Bmatrix}$$

$$u_d(t) = f_d(t) \quad u_c(t) = f_c(t).$$

In the present analysis, the form expressed by equation (1a) is used in the Newmark scheme whereas that by equation (1b) is used in a SIMULINK model for the Runge-Kutta scheme.

### *2.2. The Model of the Actuator*

The actuator model (Figure 1) is expressed by the following algebraic function, nonlinear in actuator current and present gap between the structure/rotor and actuator:

$$f_a(t) = \frac{k'i(t)^2}{y_g(t)^2} = \frac{k'i(t)^2}{(y_0 - y(t))^2} \tag{2}$$

where the actuator force is denoted by $f_a(t)$, the current in the actuator coil by $i(t)$ and the present gap between the structure/rotor and the actuator by $y_g(t)$. The proportionality constant $k'$ depends on the dimension of the electromagnet, its material and the number of turns of the coil.

The initial gap between the structure/rotor and the actuator, when the structure/rotor is in a static condition and there is no current through the actuator coil, is denoted by $y_0$. The displacement of the structure/rotor is measured from this position.

Becausee the actuator force is proportional to the square of the current, irrespective of positive or negative current in the actuator, the actuator will always produce a pulling force.

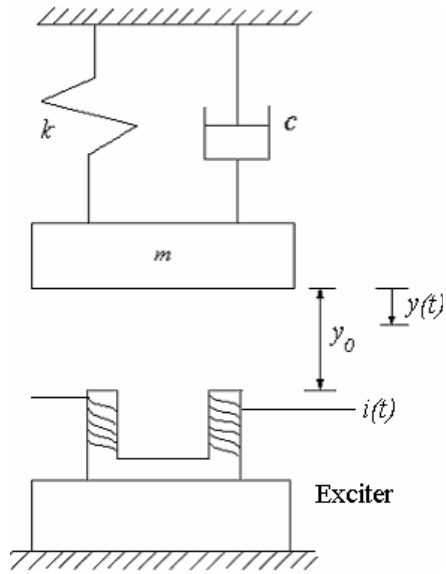


Figure 1. The single-degree-of-freedom system with one-sided magnetic actuator.

For the purpose of control, in the present exercise, the actuator current is not allowed to become negative. In the absence of any disturbance applied to the structure/rotor, there is always a constant current in the actuator coil. This constant current always makes the structure/rotor (on which the actuator is working) remain in a constant deformed configuration. In magnetic bearing terminology, this constant current is known as the bias current.

When the magnetizing current is constant, the actuator force is inversely proportional to the square of the displacement except for a small region very close to the magnet (Schweitzer et al., 2003). There is a scope for exploring a better model for the actuator, which is valid over a larger range of operation.

### *2.3. Digital Proportional-Derivative (PD) Control*

The plant with the digital controller is shown in Figure 2(a).

As mentioned earlier, the structure/rotor along with actuator and sensor is continuous in time. This implies that the input to the plant, its output and the states are all continuous functions of time. On the other hand, the controller is a digital one and hence it works on digital data, i.e. a series of discrete values obtained by sampling a signal, continuous in time, at regular sampling intervals.

Here, a digital proportional derivative (PD) control technique is used for vibration control of the structure/rotor. The sensor and the actuator are collocated.

The displacement signal from the sensor is sampled at a specific interval of time ($T$) and is made available to the digital controller by an analog to digital converter (ADC). In continuous PD control (Figure 2(b)), the present values of displacement $y\,(t)$ and velocity $\dot{y}\,(t)$ at the location of the actuator determine the control force $f_c\,(t)$ at all instants of time.

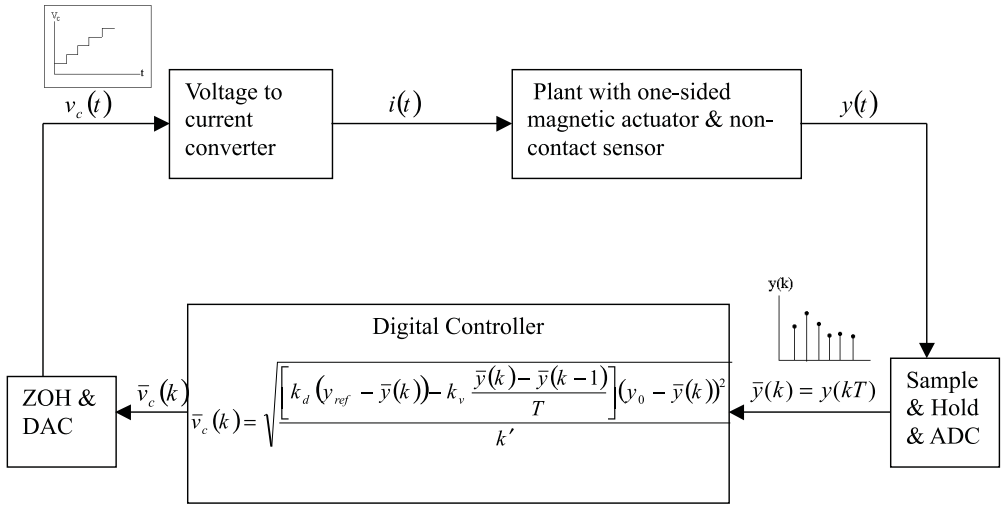


(a)

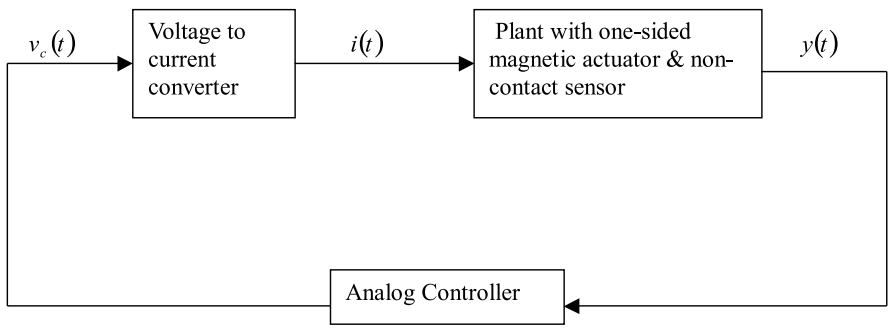


(b)

Figure 2. (a) The block diagram shows digital PD control using one-sided magnetic actuator. The DAC and ADC are in most cases an integral part of the digital controller. (b) The block diagram shows continuous-time control using one-sided magnetic actuator. The analog controller should supply an appropriate continuous voltage signal determined using analog electronic circuitry.

$$f_c(t) = k_d\left(y_{ref} - y(t)\right) - k_v\dot{y}(t) \tag{3}$$

where the proportional and derivative gains are represented by $k_d$ and $k_v$ respectively.

The reference $y_{ref}$ is a positive constant, which always produces a positive displacement. When performing the control action, this reference value can be adjusted to prevent negative actuator current.

In digital control, to compute the control force at an instant, the following method is adopted. If the present time $t$ be an intermediate time between the $(k-1)\,th$ and $kth$ samples

$$(k-1)\,T < t < kT.$$

The control force $f_c(t)$ would be computed as follows:

$$f_c(t) = k_d\left(y_{ref} - \bar{y}(k-1)\right) - k_v \frac{\bar{y}(k-1) - \bar{y}(k-2)}{T} \qquad (k-1)\,T < t < kT \quad (4)$$

where $\bar{y}(k)$ is the sampled value of $y(t)$ at time $t = kT$.

However, the input to the actuator is a continuous current. An appropriate value of current in the actuator coil should generate the above actuator force. The value of current is computed based on a standard model of the nonlinear actuator given by equation (2).

The digital controller generates a voltage signal $\bar{v}_c(k-1)$ proportional to the value of the control current at the sampling instant $t = (k-1)\,T$.

Between two consecutive sampling instants, $t = (k-1)\,T$ and $t = kT$, the value of this control signal is kept constant by using a ZOH. This staircase-type continuous control signal $v_c(t)$ is available from the DAC. Therefore, in digital control, the control signal changes in steps.

A voltage to current converter produces a current $i(t)$ proportional to the voltage signal. This current is fed to the actuator coils to produce the control force $f_c(t)$. Though the current is constant within a sampling interval, the control force is not. The changing gap between the actuator and the structure/rotor, even within a sampling interval, is the cause for this.

The working of the control loop can be described in the following steps:

1. Sample sensor output using an ADC at $(k-1)th$ instant, i.e. $t = (k-1)\,T$ and get $\bar{y}(k-1)$ as displacement at the location of the actuator.
2. Compute velocity at the location of the actuator as $\dot{\bar{y}}(k-1) = \frac{y(k-1)-y(k-2)}{T}$
3. The proportional derivative control force at the location of the actuator at this instant is $f_c(k-1) = k_d\left(y_{ref} - \bar{y}(k-1)\right) - k_v\dot{\bar{y}}(k-1)$, $(k-1)\,T < t < kT$.
   The required current at this instant can be found out using equation (2).
   Therefore, $\bar{v}_c(k-1) = \sqrt{\frac{\left\{k_d\left(y_{ref}-\bar{y}(k-1)\right)-k_v\dot{\bar{y}}(k-1)\right\}(y_0-\bar{y}(k-1))^2}{k'}}$
4. Send this voltage signal through DAC via a ZOH. Now, $v_c(t) = \bar{v}_c(k-1)$, $(k-1)T < t < kT$
5. This voltage signal is fed into a voltage to current converter of gain $1A/V$
6. The current from the voltage to current converter is sent to the actuator coil

### *2.4. The Plant (Structure/Rotor) with Actuator and Sensor*

The structure/rotor is considered here as the plant. The input to the actuator is the current to be fed to the coil of the actuator. The actuator applies force on the structure/rotor. The output of the plant is the displacement(s) at the sensor location(s). The plant, the actuator and the sensor(s) are all continuous in time. When a single actuator is used for the purpose of control, equation (1a) can be written as follows:

$$[M]\left\{\ddot{Y}(t)\right\} + [D]\left\{\dot{Y}(t)\right\} + [K]\{Y(t)\} = \{T_d\}\,f_d(t) + \{T_c\}\frac{k'i(t)^2}{y_g(t)^2}. \qquad (5)$$

Now, if it is considered that $i\,(t)$ is known (the computation of $i\,(t)$has already been described in the previous section), there is one difficulty in the numerical solution of equation (5). Since the present value of the gap $y_g\,(t)$ between the structure and the actuator depends on the present value of the displacement (element of $\{Y\,(t)\}$ at the relevant degree-of-freedom at the actuator location), the second term in the right hand side of equation (5), i.e. the control force is nonlinear.

### *2.5. Newmark Scheme with Modification for Nonlinear Actuator Force*

According to the Newmark scheme, the solution of equation (3) at present time $t$ can be obtained by solving the following simultaneous algebraic equation (Bathe, 2002):

$$\left[\bar{K}\right]\{Y\,(t)\} = \{R\,(t)\} \tag{6}$$

where,

$$\begin{aligned}
\{R\,(t)\} &= \{T_d\}\,f_d\,(t) + \{T_c\}\,\frac{ki\,(t)^2}{y_g\,(t)^2} + \textit{Other terms}\\
\textit{Other terms} &= [M]\left(a_0\{Y\,(t-\Delta t)\} + a_2\left\{\dot{Y}\,(t-\Delta t)\right\} + a_3\left\{\ddot{Y}\,(t-\Delta t)\right\}\right)\\
&+ [D]\left(a_1\{Y\,(t-\Delta t)\} + a_4\left\{\dot{Y}\,(t-\Delta t)\right\} + a_5\left\{\ddot{Y}\,(t-\Delta t)\right\}\right).
\end{aligned}$$

The values of the constants $a_0, a_1, a_2, a_4$ and $a_5$ can be found in standard texts (Bathe, 2002).

The matrix $\left[\bar{K}\right]$ can be computed from the matrices $[M]$, $[D]$, $[K]$. The vector $\{R\,(t)\}$ can be computed from disturbance and control force at the present time step, the matrices $[M]$ and $[C]$ and the values of displacement, velocity and acceleration at the previous time step. Equation (6) is solved iteratively. The solution of equation (6) can be started with the value of the gap for the previous time step ($y_g\,(t) = y_g\,(t-\Delta t)$). Then the gap value is improved upon iteratively as long as the chosen convergence criterion is not fulfilled. The algorithm can be stated in steps as follows:

A sampling interval $(k-1)\,T < t < kT$ is considered. This sampling interval is divided in several time steps $\Delta t$ for the Newmark scheme

1. Assume $\{Y\,(t)\} = \{Y(t-\Delta t)\}$
2. Find out $y_g\,(t)$ from $\{Y(t)\}$, It is shown in Figure 1 that $y_g\,(t) = y_0 - y\,(t)$ ($y(t)$ is the displacement at the relevant degree-of-freedom and an element in the vector $\{Y(t)\}$)
3. Get disturbing force $f_d(t)$
4. Compute $f_c(t) = \frac{k'i(t)^2}{y_g(t)^2}$, $i\,(t)$ remains constant during the whole of present sampling period $(k-1)\,T < t < kT$ but the gap $y_g\,(t)$ changes even within the sampling interval
5. Form right hand side of equation (6), i.e. $\{R\,(t)\} = \{T_d\}\,f_d\,(t) + \{T_c\}\,\frac{ki_c(t)^2}{y_g(t)^2} +$ *Other terms*. The values of the other terms can be computed from values of the relevant quantities already known from the previous time step
6. Get $\{Y\,(t)\} = \left[\bar{K}\right]^{-1}\{R\,(t)\}$
7. If $\|Y\,(t) - Y\,(t-\Delta t)\| > \varepsilon$, go to step 2; otherwise go to step 8

8. Increment $t$ to $t + \Delta t$
9. Go to step 1 until the final time for the present sampling interval is reached

The correction for the nonlinearity in the actuator force is accomplished in an iterative way. Step 7 checks for the convergence of the displacement. If the convergence criterion is not satisfied, steps from step 2 to step 7 are repeated. It is also possible to use a convergence criterion based on the value of the control force.

## 3. NUMERICAL EXAMPLES

Three examples are considered. The first two deal with vibration control of structures. In the third one, a rotor with a non-central disc is considered. Collocated sensor actuator pairs are employed in all of the examples. A single actuator is used in the first two examples whereas two actuators are used in the third one. The sampling time is gradually reduced to observe its effect on the response due to a step load (for structure) and a harmonic excitation (for structure and rotor).

### *3.1. Vibration Control of Single-Degree- of-Freedom System*

The model of the plant is now the same as that shown in Figure 1. The values of mass, stiffness and damping ratio for the single-degree-of-freedom system (plant) are 0.002 $\mathrm{Ns}^2/\mathrm{mm}$ (2 kg), 110 N/mm and 1% respectively. The natural frequency is approximately 234 rad/s (37 Hz).

The force on the mass at its displaced condition is

$$f_a(t) = \frac{ki(t)^2}{(y_0 - y(t))^2} \tag{7}$$

The initial gap $y_0$ between the actuator and the mass in the undeformed condition of the plant is taken as 1 mm.

The control force is

$$f_c(t) = k_d\left(y_{ref} - \bar{y}(k-1)\right) - k_v\dot{\bar{y}}(k-1), \qquad (k-1)T < t < kT.$$

The proportional gain $k_d = 50$ N/mm

The reference displacement is taken to be 1 mm

For digital control with a sufficiently small sampling interval or for analog control (continuous time), the controlled system will have a natural frequency of $\sqrt{\frac{(k+k_d)}{m}}$ rad/s. The derivative gain is so chosen that the controller impart a value of 5% damping ratio.

The derivative gain $k_v = 2 \times \sqrt{(110 + 50) \times 0.002} \times 0.05$ Ns/mm

The controlled system is suddenly subjected to a step load of $10N$. The system response

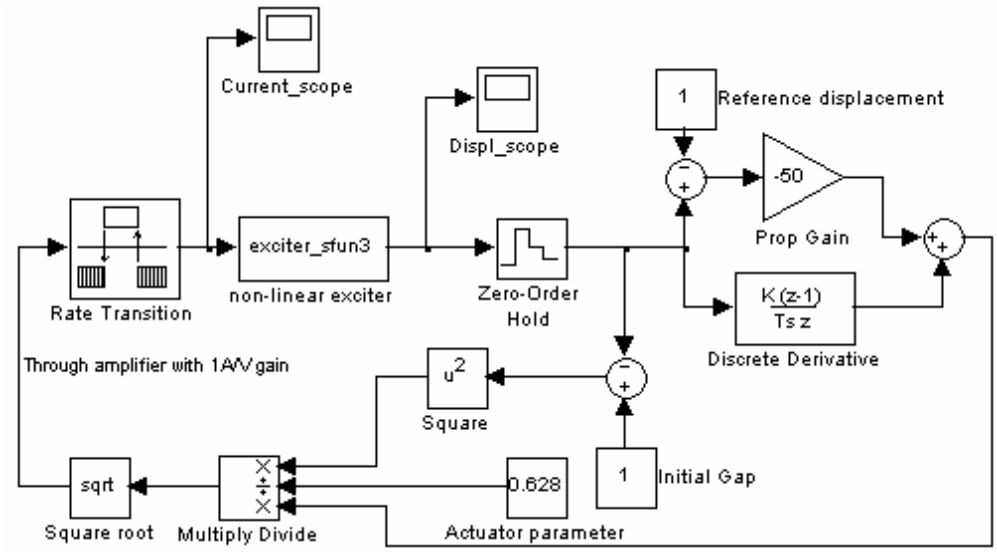


Figure 3. SIMULINK model for digital control of single-degree-of-freedom system using one-sided magnetic actuator.

with the digital PD control system is simulated using the Newmark scheme and a SIMULINK model. The SIMULINK model is shown in Figure 3. The response is computed for sampling intervals ( $T$) of 0.0005 s, 0.00025 s and 0.000125 s. The time step is taken to be $1/16^{th}$ of the sampling interval, i.e., $\Delta t = \frac{T}{16}$. The responses are shown in Figure 4(a) and Figure 4(b).

To the controlled system, the step load is applied at an intermediate time. Initially to maintain a displacement close to the reference displacement, the current in the actuator shoots up. The vibration of the plant due to this sudden increase of current slowly dies down due to damping part of the control force. Then the step load is applied to the plant causing a sudden increase of displacement. Again, the vibration due to the step load dies down with time. Figure 4 shows that only when the sampling interval is less than $T = 0.00025$ s, the response of the controlled system exhibits damping close to the value it is designed for.

The required current for vibration control due to step excitation is presented in Figure 5(a). The staircase-type pattern of input current is shown in Figure 5(b).

Figure 6 shows a plot of amplitude against frequency for a sinusoidal excitation $2.5 \sin(2\pi f t)\ N$. The response of the uncontrolled and the controlled system with sampling intervals of 0.0005s and 0.00025s are presented.

If in the algorithm presented in section 2.5, step 7 was omitted, the iterative correction for the nonlinear term would not have been performed. Then in place of solving equation (6), the following recurrence relation would have been evaluated:

$$\left[\bar{K}\right]\{Y(t)\} = \{R(t)\} \tag{8}$$

where

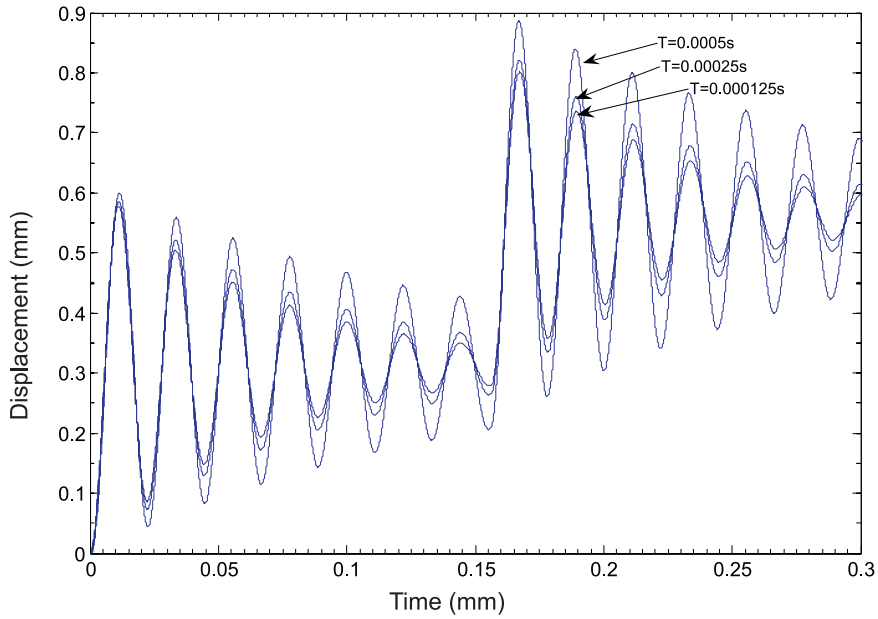


(a)

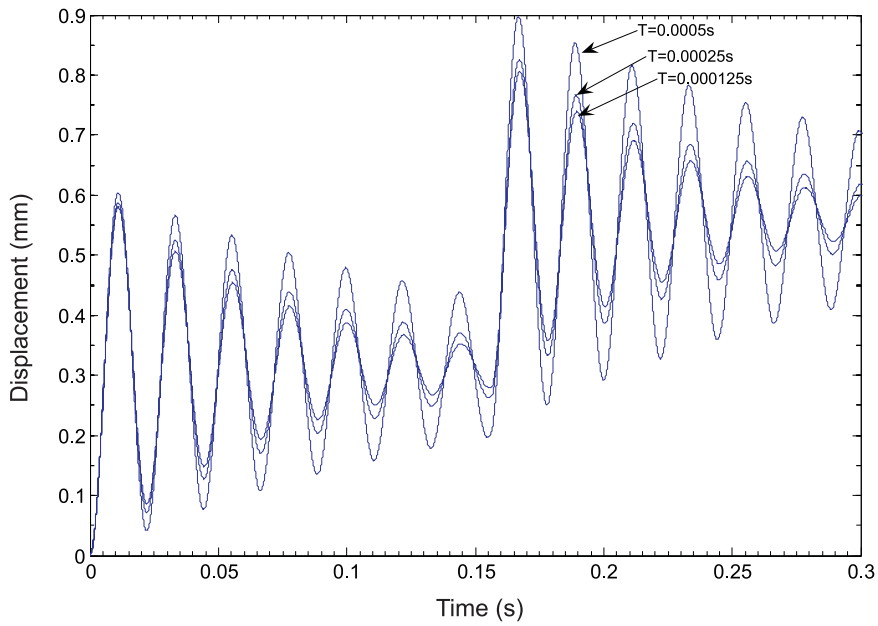


(b)

Figure 4. (a) The displacement patterns obtained for different sampling intervals. The initial vibration is due to the sudden jump in current in an attempt to reach the reference position. The second jump in displacement is due to the application of a step load of 10 N. (b) The same plot as Figure 4(a). Here the dynamic system is simulated using the SIMULINK model shown in Figure 3.

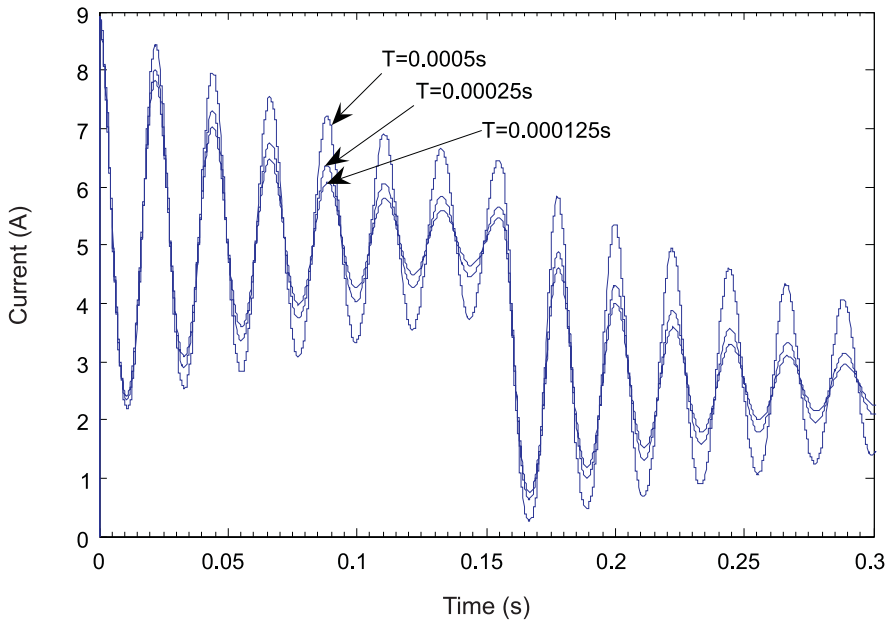


(a)

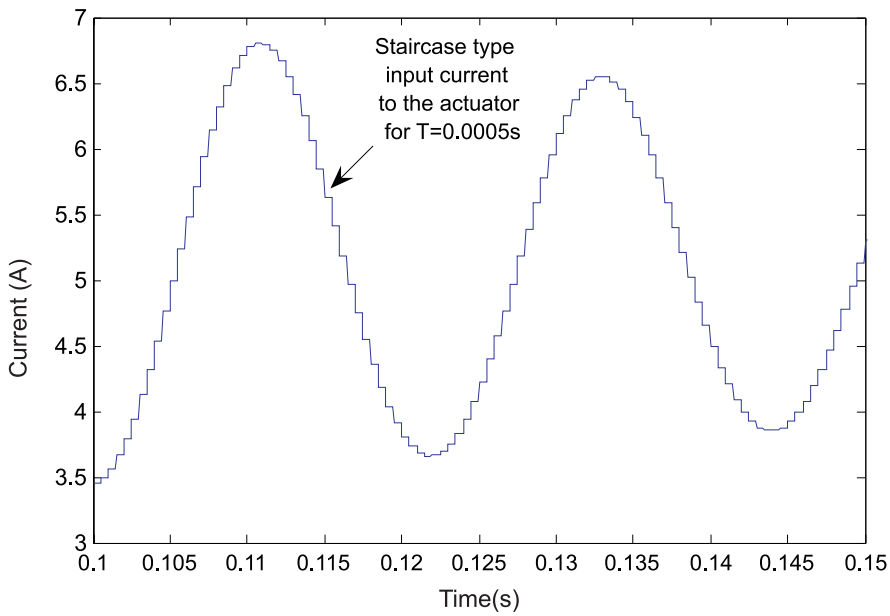


(b)

Figure 5. (a) The input current in the actuator coil for the single-degree-of-freedom system. (b) The staircase-type pattern of the input current in the actuator coil for the single-degree-of-freedom system.

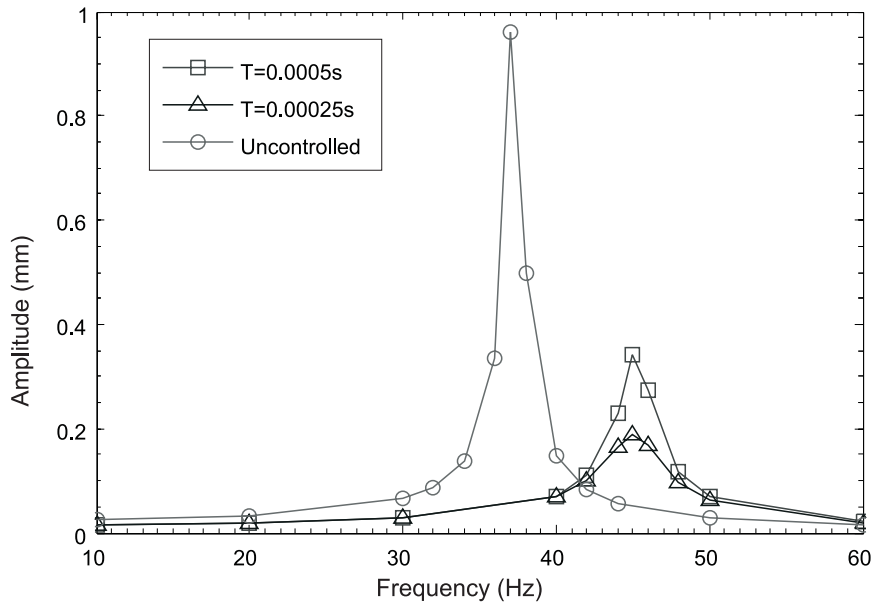


Figure 6. Amplitude versus frequency plot of the single-degree-of-freedom system subjected to a sinusoidal load of $2.5 \sin(2\pi f t)\ N$.

$$\{R(t)\} = \{T_d\}\, f_d(t) + \{T_c\} \frac{ki(t)^2}{y_g(t - \Delta t)^2} + \textit{Other terms.}$$

If equation 8 is solved, it is expected that an erroneous solution would be obtained. The error would increase with the increase in sampling interval. For a sampling interval of $T = 0.00075$ s, the solutions, with and without the correction for a nonlinear actuator force, are presented in Figure 7.

### *3.2. Vibration Control of a Beam Using One-Sided Magnetic Actuator*

This example (Figure 8) is very similar to the previous one except for the fact that a finite element model of a lightly damped beam is now used to demonstrate the performance of the one-sided actuator. The beam is made up of steel, 600 mm in length and 15 mm in diameter. The beam is simply supported at its two ends. Apart from the distributed mass of the beam, a concentrated mass of 0.002 $\mathrm{Ns}^2/\mathrm{mm}$ (2 kg) is placed at the mid-span of the beam. The beam is subjected to a disturbance of $10 \sin(2\pi 40t)\ N$ at a distance of a quarter of the length from one side. A collocated sensor and one-sided magnetic actuator are placed at the middle of the beam.

A finite element model of the beam, consisting of four elements with equal lengths, is considered. The values of the proportional and derivative gains and the reference displacement are the same as those used in the previous example. The value of $k'$ for the actuator also remains the same. The Newmark scheme, with appropriate modification for force nonlinearity, is used for the purpose of computing the response of the beam. The time step for

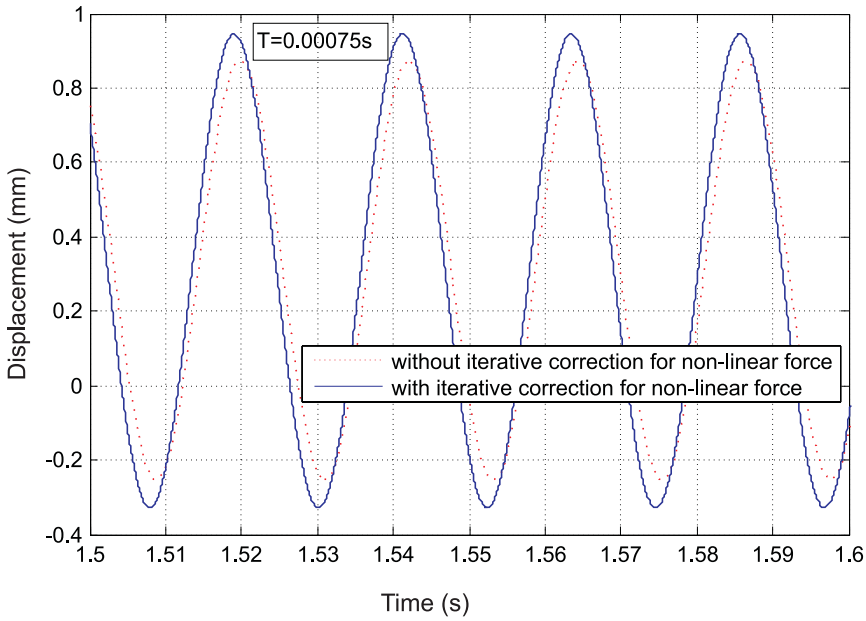


Figure 7. The effect of iterative correction for nonlinear actuator force for a harmonic excitation load of $2.5 \sin(2\pi f t)\ N$.

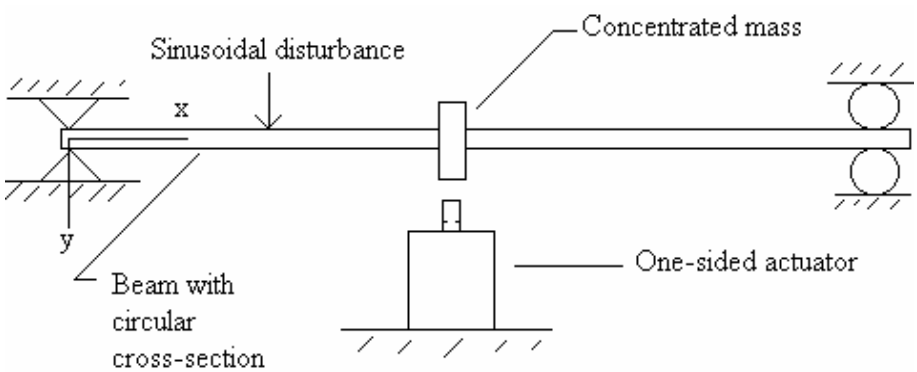


Figure 8. A beam with collocated sensor and one-sided magnetic actuator.

the Newmark scheme is 1/16th of the sampling interval. Three different sampling intervals of 0.0005 s, 0.00025 s and 0.000125 s are considered. The responses are presented in Figure 9(a). For the sampling interval of 0.0005 s, the beam displacement is found to increase and hit the actuator. For the other two sampling intervals the responses are quite close. The frequency response of the beam with and without the actuator is shown in Figure 9(b). This figure demonstrates the performance of the one-sided magnetic actuator.

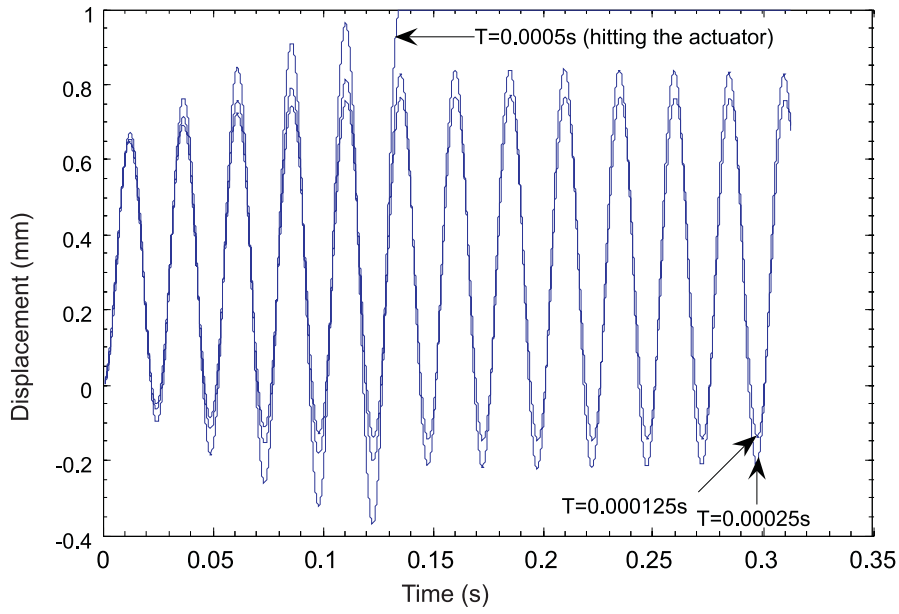


(a)

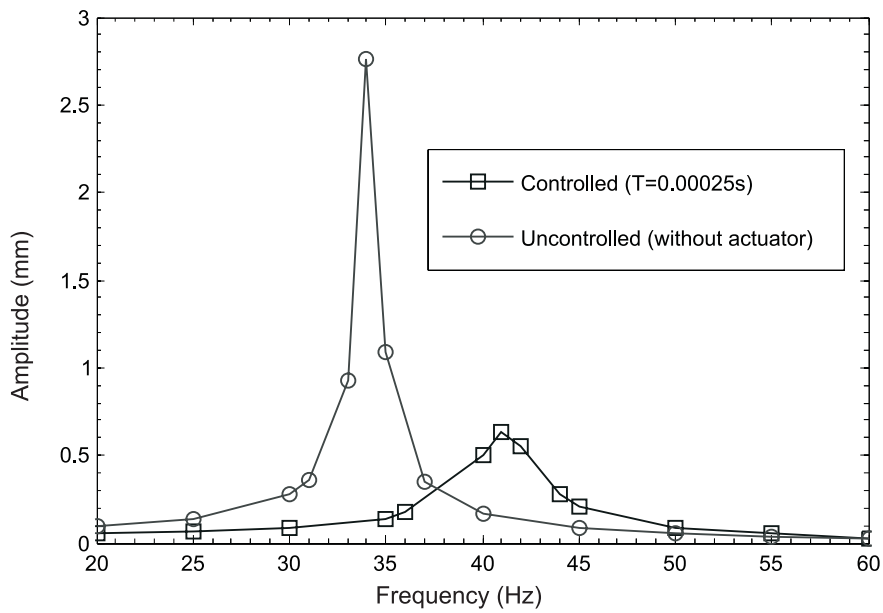


(b)

Figure 9. (a) The response of the beam subjected to a sinusoidal excitation $10\sin(2\pi 40t)\ N$. (b) Frequency response of the beam with and without the magnetic actuator.

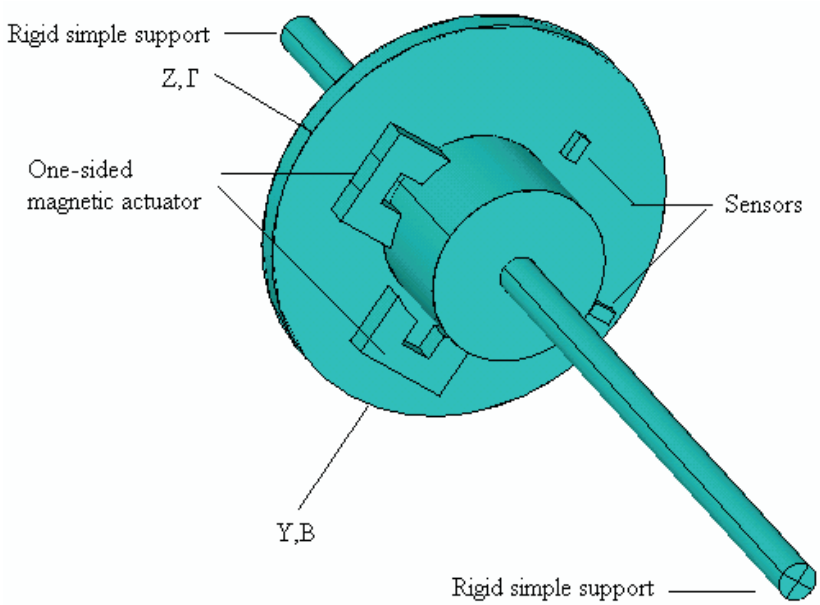


Figure 10. Schematic diagram showing a rotor with a non-central disc with one-sided magnetic actuator close to the disc.

### *3.3. Vibration Control of a Rotor Using One-Sided Magnetic Actuator*

Figure 10 shows a schematic diagram for this example. In this example a shaft with a non-central disc is analyzed. The shaft has two rigid simple supports (self-aligning rolling element bearings can be modeled as simple supports) at its two ends. The supports are much more rigid compared to the shaft. The shaft has a diameter of 15 mm. The length of the shaft is $l = 600$ mm. The mass of the shaft is not considered. The non-centrally placed disc is thin and has a mass of 0.002 $\text{Ns}^2/\text{mm}$ (2 kg). The disc is placed at a distance of $0.35l$ from one end of the shaft. The radius of gyration for the polar moment of inertia of the disc is $0.4l$. The disc has an unbalance of $me = 0.25 \times 10^{-4}$ kg $- m$. The moment of inertia about the diameter is half of the polar moment of inertia. Two one-sided magnetic actuators and two sensors are placed close to the disc. The actuators and the sensors are collocated.

A four degree-of-freedom model of the lightly damped rotor is analyzed. The mass, gyroscopic and stiffness matrices for this model are available from standard texts (Kramer, 1993).

The imaginary and real parts of the eigenvalues of the open loop system (rotor without any control system) are computed and plotted in Figure 11. In this example, the unbalance excitation at the location of the disc is considered as the sole source of disturbance. It is known that unbalance excitation of rotor on isotropic supports can only excite the forward whirl modes. The approximate location of the first critical speed for the uncontrolled rotor is indicated in Figure 11.

For the controlled rotor, the values of the proportional and derivative gains and the reference displacement are the same as those used in previous examples. The value of $k'$ for the

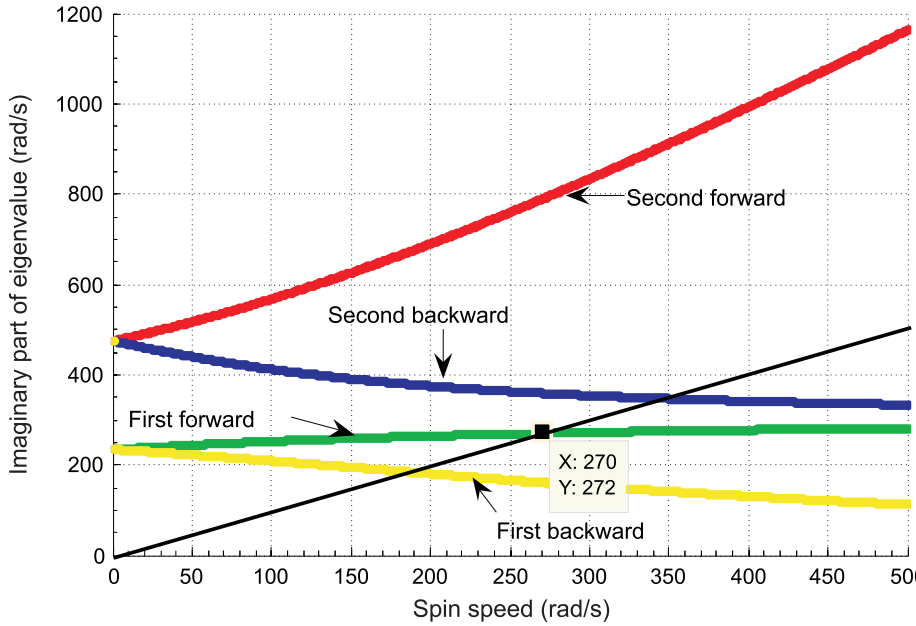


(a)

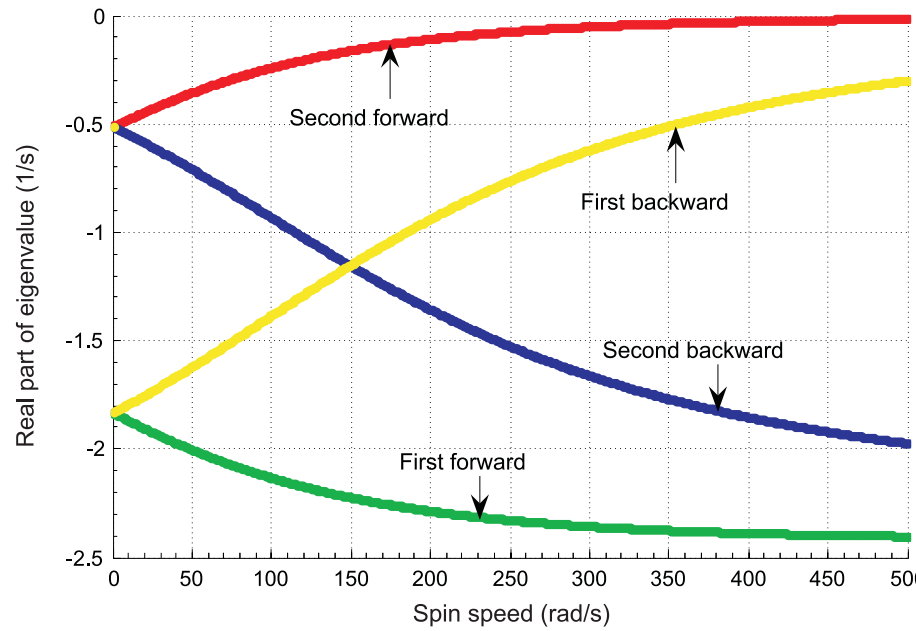


(b)

Figure 11. (a) The imaginary part of the eigenvalues of the uncontrolled rotor. (b) The real part of the eigenvalues of the uncontrolled rotor.

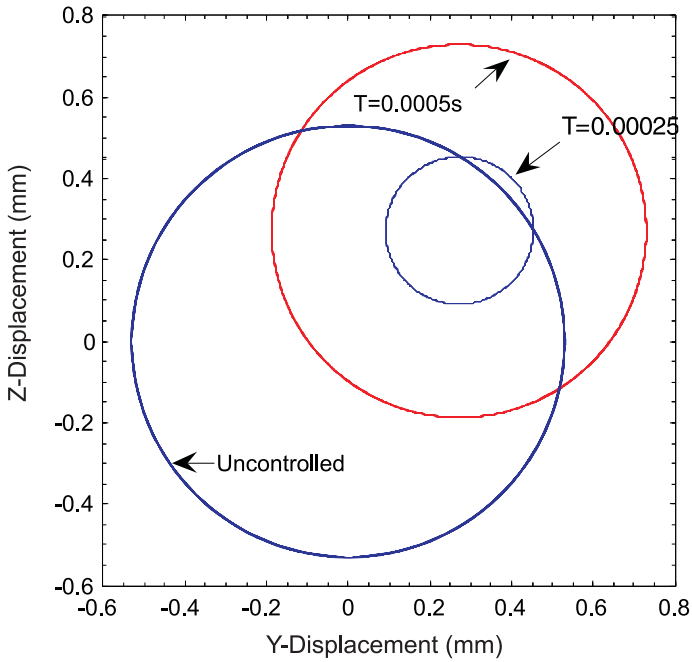


(a)

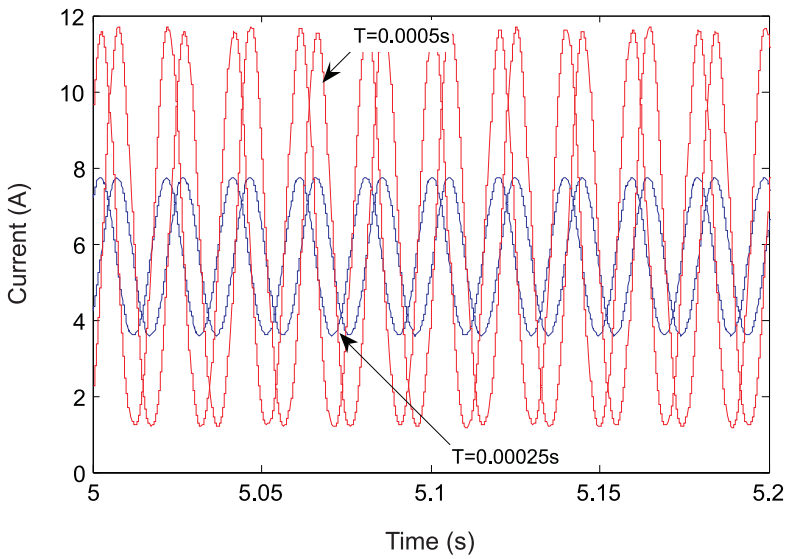


(b)

Figure 12. (a) Orbits computed at spin speeds close to corresponding critical speeds. For the uncontrolled rotor a spin speed of $270\ \mathrm{rad/s}$ is considered. For the controlled one, the orbit is computed at a spin speed of $320\ \mathrm{rad/s}$ for two different sampling intervals. (b) The input current in the actuator coils (two actuators for two perpendicular directions) for the controlled rotor for two different sampling intervals.

actuator also remains the same. The Newmark scheme, with modification for force nonlinearity, is used for the purpose of computing the response of the rotor. The time step for the Newmark scheme is 1/8th of the sampling interval.

The orbit of the uncontrolled and the controlled rotor are plotted in Figure 12(a). The uncontrolled and the controlled rotor have different critical speeds. Here, the orbits are computed at a spin speed close to the critical speed. For the uncontrolled rotor a spin speed of 270 rad/s is considered. For the controlled rotor, the orbit is computed at a spin speed of 320 rad/s. For the controlled rotor, two different sampling intervals of 0.0005 s and 0.00025 s are considered. It is observed that the orbit computed with the smaller sampling interval is considerably less than that computed using the larger one. The required current inputs for the two actuators are shown in Figure 12(b).

## 4. CONCLUSION

It has been shown that for the problem considered, a value of the sampling interval can be obtained from a reasonably accurate numerical simulation. For all the numerical examples, the value of the sampling interval for a satisfactory response is found to be sufficiently smaller than that of LTI systems. Selection for the hardware largely depends on this estimated sampling interval. For a more accurate simulation, the model for the voltage to current converter should also be introduced in the system model. The quantization error in the process of analog to digital conversion is neglected on the assumption that a 16-bit data acquisition system has been used. However, at the end, the effectiveness of the present exercise can only be verified in an actual implementation.

*Acknowledgement. The first two authors are grateful to TEQIP (Technical Education Quality Improvement Programme) of the government of India for funding their visit to the Institute for Mechanics, University of Kassel, Germany. The authors are also grateful to Jadavpur University authorities for their help and support. The first author acknowledges the partial funding of the work by the Department of Science and Technology, government of India (No. SR/FTP/ETA-32/2003). The authors acknowledge the support of all their colleagues and staff in the Institute for Mechanics, University of Kassel.*

## REFERENCES

Bathe, K. J., 2002, *Finite Element Procedures*, Prentice Hall of India, New Delhi.

Chiba, A., Fukao, T., Ichikawa, O., Oshima, M., Takemoto, M., and Dorell, D., 2005, *Magnetic Bearings and Bearingless Drives*, Newnes, Burlington, MA.

Genta, G., 2004, *Dynamics of Rotating Systems*, Springer, New York.

Gopal, M., 2003, *Digital Control Engineering*, New Age International Publishers, New Delhi.

Kramer, E., 1993, *Dynamics of Rotors and Foundations*, Springer-Verlag, Heidelberg.

Kreuzinger-Janik, T. and Irretier, H., 2000a, "Experimental modal analysis – a tool for unbalance identification of rotating machines," *International Journal of Rotating Machinery* **6(1)**, 11–18.

Kreuzinger-Janik, T. and Irretier, H., 2000b, "Unbalance identification of flexible rotors based on experimental modal analysis," in *7th International Conference on Vibrations in Rotating Machinery,* Nottingham, UK, September 12–14.

Schweitzer, G., Bleuler, H., and Traxler, A., 2003, *Active Magnetic Bearings*, Authors' Reprint, Zurich.